

NUMERICAL SOLUTION OF HALL EFFECT ON MHD MIXED CONVECTION FLOW  
PAST AN INFINITE VERTICAL POROUS PLATE WITH MASS TRANSFER  
IN PRESENCE OF CHEMICAL REACTION

Y. DHARMENDAR REDDY\*, V. SRINIVASA RAO

Department of Mathematics,  
Anurag Group of Institutions, Ghatkesar, R. R. Dist., Telangana State, India.

(Received On: 14-08-16; Revised & Accepted On: 16-09-16)

---

ABSTRACT

*The objective of this work is to study chemical reaction and mass transfer on an unsteady hydro-magnetic flow of a radiative vertical porous plate, taking the effect of Hall current into account. Dimensionless governing equations of the problem have been solved by using finite element technique and the solutions are obtained for velocity, temperature and concentration distributions as well as for the shearing stress, rate of heat and mass transfer at the wall. The influence of the various parameters like Radiation parameter, Hall parameter, Chemical Reaction parameter, Hartmann number, frequency parameter etc. on the flow field are presented, the results obtained are discussed with the help of graphs and tables to observe effect of various parameters concerned in the problem under investigation.*

**Keywords:** Hall Effect, Chemical Reaction, MHD, Radiation, Mass transfer, Finite Element Method.

---

INTRODUCTION

Convective flows with simultaneous heat and mass transfer under the influence of a magnetic field and chemical reaction arises in many transport processes both naturally and artificially in many branches of science and engineering applications. This phenomenon plays an important role in the chemical industry, power and cooling industry for drying, chemical vapour deposition on surfaces, cooling of nuclear reactors and petroleum industries. Natural convection flow occurs frequently in nature. It occurs due to temperature differences, as well as due to concentration differences or the combination of these two, for example in atmospheric flows, there exists differences in water concentration and hence the flow is influenced by such concentration difference.

In nature, the presence of pure air or water is not possible. Some foreign mass may be present naturally mixed with air or water. The presence of foreign mass in air or water causes some kind of chemical reaction. The study of such type of chemical reaction processes is useful for improving a number of chemical technologies, such as food processing, polymer production and manufacturing of ceramics or glassware.

The fluid flows with chemical reaction have attracted the attention of engineers and scientists in the recent times. Such flows have key importance in many processes including drying evaporation at the surface of a water body, energy transfer in a wet cooling tower, flow in a desert cooler, generating electric power, food processing, groves of fruit trees, and crops damage because of freezing. There is always a molecular diffusion of species in the presence of chemical reaction within or at the boundary during several practical diffusive operations. There are two types of reactions, namely, homogeneous and heterogeneous. A homogeneous reaction takes place uniformly in the entire given phase whereas a heterogeneous reaction exists in a restricted region or within the boundary of a phase. The smog formation is an important example representing a first-order homogeneous chemical reaction. Several researchers in view of such facts are engaged in the discussion of flows with chemical reactions. Anand Rao *et.al* [1] studied the Chemical Reaction Effects on an Unsteady MHD Free Convection Fluid Flow past a Semi-Infinite Vertical Plate Embedded in a Porous Medium with Heat Absorption. S. Ahmed and K. Kalita [2] discussed the MHD Radiating Flow over an Infinite Vertical Surface Bounded by a Porous Medium in Presence of Chemical Reaction. B. Venkateswarlu and P. V. Satya Narayana [3] analyzed Chemical reaction and radiation absorption effects on the flow and heat transfer of a nanofluid in a rotating system. Srinivasa Raju *et.al* [4] studied the chemically reacting fluid flow induced by an exponentially accelerated infinite vertical plate in a magnetic field and variable temperature via LTT and FEM. F.S. Ibrahim *et.al* [5]

---

**Corresponding Author: Y. Dharmendar Reddy\*, Department of Mathematics,  
Anurag Group of Institutions, Ghatkesar, R. R. Dist., Telangana State, India.**

examined the Effect of the chemical reaction and radiation absorption on the unsteady MHD free convection flow past a semi infinite vertical permeable moving plate with heat source and suction. B. R. Rout *et.al* [6] describes the Effect of Radiation and Chemical Reaction on Natural Convective MHD Flow through a Porous Medium with Double Diffusion. R.S. Tripathy *et.al* [7] discussed the Chemical reaction effect on MHD free convective surface over a moving vertical plate through porous medium. P.V.Satya Narayana and D.Harish Babu [8] studied the MHD heat and mass transfer of a Jeffrey fluid over a stretching sheet with chemical reaction and thermal radiation.

Natural convection induced by the simultaneous action of buoyancy forces resulting from thermal and mass diffusion is of considerable interest in many industrial applications such as geophysics, oceanography, drying processes and solidification of binary alloy. Soundalgekar [9], Soundalgekar *et.al* [10], Perdikis *et.al* [11], and Lin *et.al* [12] are some of the researchers who have studied the heat and mass transfer from a vertical plate. The effect of the magnetic field on free convection flows is important in liquid metals, electrolytes and ionized gases. The thermal physics of MHD problems with mass transfer is of interest in power engineering and metallurgy. Many cross galvanic and thermo magnetic effects occur in the boundary zone between hydraulics and thermal physics and they are relevant in the study of semiconductor materials. The mechanism of conduction in ionized gases in the presence of a strong magnetic field is different from that in a metallic substance. The electric current in ionized gases is generally carried by electrons which undergo successive collisions with other charged or neutral particles. In the ionized gases the current is not proportional to the applied potential except when the electric field is very weak. However, in the presence of strong electric field, the electrical conductivity is affected by the magnetic field. Consequently, the conductivity parallel to the electric field is reduced. Hence the current is reduced in the direction normal to both electric and magnetic fields. This phenomenon is known as the Hall Effect. The effect of magnetic field (without Hall Effect) on the unsteady free convection flow over an infinite vertical porous plate has been considered by Helmy [13]. The effect of Hall current on unsteady MHD free convection flow along a vertical porous plate has been studied by Acharya *et.al* [14]. The unsteady free convection flow over an infinite vertical porous plate due to the combined effects of thermal and mass diffusion along with Hall currents have been considered by Abo-elahab *et.al* [15] and Takhar *et.al* [16]. F.M. Ali *et.al* [17] analyzed the Effect of Hall current on MHD mixed convection boundary layer flow over a stretched vertical flat plate. Dulal Pal [18] discussed the Hall current and MHD effects on heat transfer over an unsteady stretching permeable surface with thermal radiation. S Sivaiah and R Srinivasa Raju [19] discussed the heat and mass transfer flow with Hall current, heat source, and viscous dissipation. Anand Rao *et.al* [20] analyzed the MHD transient flow past an impulsively started infinite horizontal porous plate in a rotating fluid with hall current. G.S. Seth *et.al* [21] studied the Unsteady MHD free convection flow with Hall effect of a radiating and heat absorbing fluid past a moving vertical plate with variable ramped temperature. S. Das *et.al* [22] discussed the Hall effects on an unsteady magneto-convection and radiative heat transfer past a porous plate.

All the above investigations are restricted to MHD flow and heat transfer problems. However, when the free convective flows occur at high temperatures, radiation effects on the flow become significant. Many processes in engineering areas occur at high temperatures and knowledge of radiative heat transfer becomes very important for the design of the pertinent equipment. Nuclear power plants, gas turbines and the various propulsion devices for aircraft, missiles and space vehicles are examples of such engineering areas. The inclusion of radiation effects in the energy equation leads to a highly non-linear partial differential equation. Radiation effect on mixed convection along an isothermal vertical plate was studied by Hossain and Takhar [23] using Roseland approximation while Abo-elahab [24] discussed this problem using Cogley Vincentine-Giles equilibrium model. Muthucumaraswamy *et.al* [25] discussed the heat and mass transfer effects on moving vertical plate in the presence of thermal radiation. N. Vedavathi *et.al* [26] studied the Radiation and mass transfer effects on unsteady MHD convective flow past an infinite vertical plate with Dufour and Soret effects. R.N. Barik and G.C. Dash [27] discussed the Thermal radiation effect on an unsteady magnetohydrodynamic flow past inclined porous heated plate in the presence of chemical reaction and viscous dissipation. J. Prakash *et.al* [28] analyzed the Diffusion-Thermo and Radiation Effects on Unsteady MHD Flow Through Porous Medium Past an Impulsively Started Infinite Vertical Plate with Variable Temperature and Mass Diffusion. F.I. Alao *et.al* [29] discussed the Effects of thermal radiation, Soret and Dufour on an unsteady heat and mass transfer flow of a chemically reacting fluid past a semi-infinite vertical plate with viscous dissipation.

Motivated by the above reference works and the numerous possible industrial applications of the problem, it is of paramount interest in this study to investigate the effects of radiation heat absorption and mass transfer on the flow of fluid past an infinite vertical porous plate taking chemical reaction and Hall Effect into the account.

## **MATHEMATICAL ANALYSIS**

We consider the unsteady free convection flow of a viscous, incompressible, electrically conducting fluid on an infinite vertical permeable plate located at the plane  $y' = 0$ . The  $x'$  - axis is chosen along the plate in the upward direction and  $y'$  - axis is taken perpendicular to the plate. Initially, the temperature of the plate and the fluid is assumed to be same. At time  $t > 0$ , the plate starts moving with a velocity  $ct'$  in its own plane and its temperature is instantaneously raised or lowered to  $T$  which is thereafter maintained constant. Since the plate is infinite in length, all physical quantities are

function of  $y'$  and  $t'$  only. Hence, if the velocity  $V$  is given by  $(u', v', w')$ , the equation of continuity, on integration gives

$$v' = \text{constant} = -v'_0 \text{ (say);}$$

Where  $v'_0$  is the constant normal velocity of suction or injection at the plate according to  $v'_0 > 0$  or  $< 0$  respectively.

Again if  $B = (B_x, B_y, B_z)$ , the divergence equation of the magnetic field gives

$$B_y = \text{constant} = B_0 \text{ (say);}$$

Where  $H_0$  is the externally applied transverse magnetic field. Using the relation  $\nabla \cdot J = 0$  for the current density  $J = (J_x, J_y, J_z)$ , we get  $J_y = \text{constant}$ .

Since the plate is non-conducting  $J_y = 0$  at the plate and hence zero every where. The magnetic Reynolds number of the flow is taken to be small enough so that the induced magnetic field can be neglected.

When the strength of magnetic field is very large the generalized Ohm's law, in the absence of electric field takes the following form:

$$J + \frac{\omega_e \tau_e}{B_0} (J \times B) = \sigma \left( (V \times B) + \frac{1}{en_e} \nabla P_e \right) \quad (1)$$

Where  $V$  is the velocity vector,  $\sigma$  is the electrical conductivity,  $\mu_e$  is the magnetic permeability,  $\omega_e$  is the electron frequency,  $\tau_e$  is the electron collision time,  $e$  is the electron charge,  $n_e$  is the number density of the electron,  $P_e$  is the electron pressure. Under the assumption that the electron pressure (for weakly ionized gas), the thermo-electric pressure and ion-slip are negligible, equation (1) becomes:

$$J_x = \frac{\sigma B_0}{1+m^2} (mu' - w') \quad \text{And} \quad J_z = \frac{\sigma B_0}{1+m^2} (mw' + u') \quad (2)$$

Where ' $u$ ' is the x-component of  $V$ , ' $w$ ' is the z-component of  $V$  and  $m (= w_e \tau_e)$  is the Hall parameter. Within the above framework, the equations which govern the flow under the usual Boussinesq's approximation are as follows:

$$\frac{\partial u'}{\partial t'} - v'_0 \frac{\partial u'}{\partial y'} = \nu \frac{\partial^2 u'}{\partial y'^2} - \frac{\sigma B_0^2}{\rho(1+m^2)} (u' + mw') + g\beta(T' - T'_\infty) + g\beta^*(C' - C'_\infty) \quad (3)$$

$$\frac{\partial w'}{\partial t'} - v'_0 \frac{\partial w'}{\partial y'} = \nu \frac{\partial^2 w'}{\partial y'^2} - \frac{\sigma B_0^2}{\rho(1+m^2)} (w' - mu') \quad (4)$$

$$\frac{\partial(T' - T'_\infty)}{\partial t'} - v'_0 \frac{\partial(T' - T'_\infty)}{\partial y'} = \frac{k}{\rho c_p} \frac{\partial^2(T' - T'_\infty)}{\partial y'^2} - \frac{1}{\rho c_p} \left( \frac{\partial q_r}{\partial y'} \right) \quad (5)$$

$$\frac{\partial(C' - C'_\infty)}{\partial t'} - v'_0 \frac{\partial(C' - C'_\infty)}{\partial y'} = D \frac{\partial^2(C' - C'_\infty)}{\partial y'^2} - k_r'^2 (C' - C'_\infty) \quad (6)$$

By using Cogley *et.al* [26] relation, the radiative heat flux ( $q_r$ ) for the optically thin limit non-gray gas near equilibrium is given by:

$$\frac{\partial q_r}{\partial y'} = 4I(T' - T'_\infty) \quad \text{where} \quad I = \int_0^\infty K_{\lambda w} \left( \frac{\partial e_{b\lambda}}{\partial T'} \right)_w d\lambda \quad (7)$$

Here  $K_{\lambda w}$  is the mean absorption coefficient,  $e_{b\lambda}$  is Planck's function and  $T'$  is the temperature.

In equation (5) the viscous dissipation and Ohmic dissipation are neglected and equation (6) the term due to chemical reaction is assumed to be absent. Using  $T' - T'_\infty = \theta'$  in equation (5) and  $C' - C'_\infty = C^*$  in equation (6) subjecting to the initial and boundary conditions:

$$\begin{aligned} t' \leq 0: & \quad u' = 0, \quad w' = 0, \quad \theta' = 0 \quad C^* = 0 \quad \text{for all } y' \\ t' > 0: & \quad \begin{cases} u' = 0, \quad w' = 0, \quad \theta' = ae^{i\omega t'} \quad C^* = be^{i\omega t'} & \text{at } y' = 0 \\ u' = 0, \quad w' = 0, \quad \theta' = 0, \quad C^* = 0 & \text{as } y' \rightarrow \infty \end{cases} \end{aligned} \quad (8)$$

Where  $g$  is the acceleration due to gravity,  $\beta$  is the volumetric co-efficient of thermal Expansion,  $\beta^*$  is the co-efficient of volume expansion with species concentration,  $T'$  is the temperature of the fluid with in the boundary layer,  $T'_\infty$  is the

fluid temperature away to the porous wall,  $C$  is the species concentration,  $\rho, \mu, \nu, k, c_p$  are density, viscosity, kinematics viscosity, thermal conductivity, specific heat at constant pressure respectively and  $D$  is the chemical molecular diffusivity,  $\omega$  is frequency of oscillations,  $a$  and  $b$  are taken as temperature and concentration difference respectively and subscript  $\omega$  and  $\infty$  denotes the physical quantities at the plate and in the free stream respectively and using the following non-dimensional parameters:

The non dimensional quantities introduced in the equations (3) - (6) are:

$$\left. \begin{aligned} \eta &= \frac{v_o y'}{v}, t = \frac{v_o^2 t'}{4\nu}, \Omega = \frac{4\nu\omega'}{v_o^2}, u = \frac{u'}{v_o}, w = \frac{w'}{v_o}, \theta = \frac{\theta'}{a}, C = \frac{C'}{b} \\ M &= \frac{4\sigma B_0^2 \nu}{\rho v_o^2}, P_r = \frac{\mu c_p}{k}, S_c = \frac{\nu}{D}, k = \frac{k_o v_o^2}{\nu^2}, G_r = \frac{4\nu g \beta a}{v_o^3}, \\ G_c &= \frac{4\nu g \beta^* b}{v_o^3}, F = \frac{16\nu l}{v_o^2 \rho c_p}, k_r^2 = \frac{k_r'^2 \nu}{V_o^2} \end{aligned} \right\} \quad (9)$$

The governing equations can be obtained in the dimension less form as:

$$\frac{\partial u}{\partial t} - 4 \frac{\partial u}{\partial \eta} = 4 \frac{\partial^2 u}{\partial \eta^2} - \frac{M}{(1+m^2)}(u+mw) + G_r \theta + G_c C \quad (10)$$

$$\frac{\partial w}{\partial t} - 4 \frac{\partial w}{\partial \eta} = 4 \frac{\partial^2 w}{\partial \eta^2} - \frac{M}{(1+m^2)}(w-mu) \quad (11)$$

$$\frac{\partial \theta}{\partial t} - 4 \frac{\partial \theta}{\partial \eta} = \frac{4}{P_r} \frac{\partial^2 \theta}{\partial \eta^2} - F \theta \quad (12)$$

$$\frac{\partial C}{\partial t} - 4 \frac{\partial C}{\partial \eta} = \frac{4}{S_c} \frac{\partial^2 C}{\partial \eta^2} - k_r^2 C \quad (13)$$

And the boundary conditions (8) in the non-dimensional form are:

$$\begin{aligned} t \leq 0: & \quad u = 0, \quad w = 0, \quad \theta = 0, \quad C = 0 \quad \text{for all } \eta \\ t > 0: & \quad \begin{cases} u = 0, & w = 0, & \theta = e^{i\Omega t}, & C = e^{i\Omega t} & \text{at } \eta = 0 \\ u = 0, & w = 0, & \theta = 0, & C = 0 & \text{as } \eta \rightarrow \infty \end{cases} \end{aligned} \quad (14)$$

## METHOD OF SOLUTION

The Galerkin expression for the differential equation (10) becomes

$$\int_{y_j}^{y_k} \left\{ N^T \left[ 4 \frac{\partial^2 u^{(e)}}{\partial \eta^2} - \frac{\partial u^{(e)}}{\partial t} + 4 \frac{\partial u^{(e)}}{\partial \eta} - Au^{(e)} + P \right] \right\} d\eta = 0$$

$$\text{Where } N^T = [N_j \quad N_k]^T = \begin{bmatrix} N_j \\ N_k \end{bmatrix}, A = \frac{M}{1+m^2}, P = (G_r)\theta + (G_m)C - Amw;$$

Let the linear piecewise approximation solution

$$u^{(e)} = N_j(y)u_j(t) + N_k(y)u_k(t) = N_j u_j + N_k u_k$$

The element equation is given by

$$\begin{aligned} 4 \int_{y_j}^{y_k} \left\{ \begin{bmatrix} N_j' & N_j' & N_j' & N_k' \\ N_j' & N_k' & N_k' & N_k' \end{bmatrix} \begin{bmatrix} u_j \\ u_k \end{bmatrix} \right\} d\eta + \int_{y_j}^{y_k} \left\{ \begin{bmatrix} N_j & N_j & N_j & N_k \\ N_j & N_k & N_k & N_k \end{bmatrix} \begin{bmatrix} \dot{u}_j \\ \dot{u}_k \end{bmatrix} \right\} d\eta - 4 \int_{y_j}^{y_k} \left\{ \begin{bmatrix} N_j & N_j' & N_j & N_k' \\ N_j' & N_k & N_k' & N_k \end{bmatrix} \begin{bmatrix} u_j \\ u_k \end{bmatrix} \right\} d\eta \\ + A \int_{y_j}^{y_k} \left\{ \begin{bmatrix} N_j & N_j & N_j & N_k \\ N_j & N_k & N_k & N_k \end{bmatrix} \begin{bmatrix} u_j \\ u_k \end{bmatrix} \right\} d\eta = P \int_{y_j}^{y_k} \begin{bmatrix} N_j \\ N_k \end{bmatrix} d\eta \end{aligned}$$

Where prime and dot denotes differentiation w.r.to 'y' and 't' respectively Simplifying we get

$$\frac{4}{l^{(e)^2}} \begin{bmatrix} 1 & -1 \\ -1 & 1 \end{bmatrix} \begin{bmatrix} u_j \\ u_k \end{bmatrix} + \frac{1}{6} \begin{bmatrix} 2 & 1 \\ 1 & 2 \end{bmatrix} \begin{bmatrix} \dot{u}_j \\ \dot{u}_k \end{bmatrix} - \frac{4}{2l^{(e)}} \begin{bmatrix} -1 & 1 \\ -1 & 1 \end{bmatrix} \begin{bmatrix} u_j \\ u_k \end{bmatrix} + \frac{A}{6} \begin{bmatrix} 2 & 1 \\ 1 & 2 \end{bmatrix} \begin{bmatrix} u_j \\ u_k \end{bmatrix} = \frac{P}{2} \begin{bmatrix} 1 \\ 1 \end{bmatrix}$$

where  $l^{(e)} = y_k - y_j = h$

In order to get the differential equation at the knot  $x_i$ , we write the element equations for the elements  $y_{i-1} \leq y \leq y_i$  and  $y_i \leq y \leq y_{i+1}$  assemble two element equations, we obtain

$$\frac{4}{l^{(e)^2}} \begin{bmatrix} 1 & -1 & 0 \\ -1 & 2 & -1 \\ 0 & -1 & 1 \end{bmatrix} \begin{bmatrix} u_{i-1} \\ u_i \\ u_{i+1} \end{bmatrix} + \frac{1}{6} \begin{bmatrix} 2 & 1 & 0 \\ 1 & 4 & 1 \\ 0 & 1 & 2 \end{bmatrix} \begin{bmatrix} \dot{u}_{i-1} \\ \dot{u}_i \\ \dot{u}_{i+1} \end{bmatrix} - \frac{4}{2l^{(e)}} \begin{bmatrix} -1 & 1 & 0 \\ -1 & 0 & 1 \\ 0 & -1 & 1 \end{bmatrix} \begin{bmatrix} u_{i-1} \\ u_i \\ u_{i+1} \end{bmatrix} + \frac{A}{6} \begin{bmatrix} 2 & 1 & 0 \\ 1 & 4 & 1 \\ 0 & 1 & 2 \end{bmatrix} \begin{bmatrix} u_{i-1} \\ u_i \\ u_{i+1} \end{bmatrix} = \frac{P}{2} \begin{bmatrix} 1 \\ 2 \\ 1 \end{bmatrix}$$

We put the row equation corresponding to the knot 'i', is

$$\frac{4}{l^{(e)^2}} [-u_{i-1} + 2u_i - u_{i+1}] + \frac{1}{6} [\dot{u}_{i-1} + 4\dot{u}_i + \dot{u}_{i+1}] - \frac{4}{2l^{(e)}} [-u_{i-1} + u_{i+1}] + \frac{A}{6} [u_{i-1} + 4u_i + u_{i+1}] = P$$

Applying Crank-Nicholson method to the above equation then we gets

$$A_1 u_{i-1}^{n+1} + A_2 u_i^{n+1} + A_3 u_{i+1}^{n+1} = A_4 u_{i-1}^n + A_5 u_i^n + A_6 u_{i+1}^n + 12Pk \quad (15)$$

Where  $A_1 = 2 + 12rh + Ak - 24r$ ;  $A_2 = 4Ak + 48r + 8$ ;  $A_3 = 2 + Ak - 12rh - 24r$ ;  
 $A_4 = 2 - Ak - 12rh + 24r$ ;  $A_5 = 8 - 4Ak - 48r$ ;  $A_6 = 2 - Ak + 12rh + 24r$ ;

$$P = (G_r) \theta_i^j + (G_m) C_i^j - Amw_i^j;$$

Applying similar procedure to equation (11), then we gets

$$B_1 w_{i-1}^{n+1} + B_2 w_i^{n+1} + B_3 w_{i+1}^{n+1} = B_4 w_{i-1}^n + B_5 w_i^n + B_6 w_{i+1}^n + 12kQ \quad (16)$$

Where  $B_1 = 2 + 12rh + Ak - 24r$ ;  $B_2 = 4Ak + 48r + 8$ ;  $B_3 = 2 + Ak - 12rh - 24r$ ;  
 $B_4 = 2 - Ak - 12rh + 24r$ ;  $B_5 = 8 - 4Ak - 48r$ ;  $B_6 = 2 - Ak + 12rh + 24r$ ;

$$Q = Amu_i^j;$$

Applying similar procedure to equation (12), then we gets

$$G_1 \theta_{i-1}^{n+1} + G_2 \theta_i^{n+1} + G_3 \theta_{i+1}^{n+1} = G_4 \theta_{i-1}^n + G_5 \theta_i^n + G_6 \theta_{i+1}^n \quad (17)$$

Where  $G_1 = -24r + 12rhSc + kSck_r^2 + 2Sc$ ;  $G_2 = 48r + 4kSck_r^2 + 8Sc$ ;  $G_3 = -24r - 12rhSc + kSck_r^2 + 2Sc$ ;  
 $G_4 = 24r - 12rhSc - kSck_r^2 + 2Sc$ ;  $G_5 = -48r + 4kSck_r^2 + 8Sc$ ;  $G_6 = 24r + 12rhSc - kSck_r^2 + 2Sc$

Applying similar procedure to equation (13), then we gets

$$J_1 C_{i-1}^{n+1} + J_2 C_i^{n+1} + J_3 C_{i+1}^{n+1} = J_4 C_{i-1}^n + J_5 C_i^n + J_6 C_{i+1}^n \quad (18)$$

Where  $J_1 = 2Sc + 12rhSc - 24r$ ;  $J_2 = 8Sc + 48r$ ;  $J_3 = 2Sc - 12rhSc - 24r$ ;  
 $J_4 = 2Sc - 12rhSc + 24r$ ;  $J_5 = 8Sc - 48r$ ;  $J_6 = 2Sc + 12rhSc + 24r$ ;

Here  $r = \frac{k}{h^2}$  and k, h are mesh sizes along y- direction and time-direction respectively index 'i' refers to space and 'j' refers to time .The mesh system consists of  $h=0.1$  and  $k=0.001$ .

In the equations (15), (16), (17) and (18), taking  $i = 1(1)10$  and using boundary conditions in (14), then we get the following tri-diagonal system of equations

$$Au=B \quad (19)$$

$$Ew=F \quad (20)$$

$$X\theta=Y \quad (21)$$

$$LC=N \quad (22)$$

Where A, E and X are the tri-diagonal matrices of order ten and whose elements are defined by

$$\begin{aligned} A_{i,i} &= A_2; E_{i,i} = B_2; X_{i,i} = G_2; L_{i,i} = J_2 & \text{at } i = 1(1) n \\ A_{i-1,i} &= A_1; E_{i-1,i} = B_1; X_{i-1,i} = G_1; L_{i-1,i} = J_1 & \text{at } i = 2(1) n \\ A_{i,i+1} &= A_3; E_{i,i+1} = B_3; X_{i,i+1} = G_3; L_{i,i+1} = J_3 & \text{at } i = 2(1) n \end{aligned}$$

And u, B, w, F,  $\theta$ , Y, C and N are column matrices having n- components namely  $u_{i,j+1}$ ,  $B(i,j)$ ,  $w_{i,j+1}$ ,  $F(i,j)$ ,  $\theta_{i,j+1}$ ,  $Y(i,j)$ ,  $C_{i,j+1}$  and  $N(i,j)$ ;  $i=1(1)10$  respectively. The solutions of (19), (20), (21) and (22) are obtained by using Thomas algorithm. To judge the accuracy of convergence and stability of finite element scheme, the programmed was run with smaller values of k. i.e.  $k=0.005$  and no significant change was observed. Hence we conclude that the finite element scheme is stable and convergent.

**Skin friction, Rate of heat and mass transfer:**

The shearing stress at the wall along x-axis is given by  $\tau_1 = \left( \frac{\partial u}{\partial \eta} \right)_{\eta=0}$

The shearing stress at the wall along z-axis is given by  $\tau_2 = \left( \frac{\partial w}{\partial \eta} \right)_{\eta=0}$

The heat transfer coefficient in terms of Nusselt number is given by

$$Nu = \left( \frac{\partial \theta}{\partial \eta} \right)_{\eta=0}$$

The heat transfer coefficient in terms of Sherwood number is given by

$$Sh = \left( \frac{\partial C}{\partial \eta} \right)_{\eta=0}$$

**RESULTS**

In order to illustrate the influence of various parameters on the velocity, temperature, concentration fields, shearing stress, rate of heat and mass transfer, numerical calculations of the solutions, obtained in the preceding section, have been carried out for both cases corresponding to cooling and heating of the porous plate by free convection currents. Figures 1 to 5 depicts the primary velocity profiles u against  $\eta$  for cooling ( $Gr > 0$ ) and heating ( $Gr < 0$ ) of the plate by free-convection currents taking different values of F (radiation parameter), Sc (Schmidt number), M (Hartmann number), m (Hall parameter) and  $\Omega$  (Frequency parameter).

The effect of the magnetic field parameter (M) is shown in figure 1 in case of cooling of the plate. It is observed that the primary velocity of the fluid decreases with the increase of the magnetic field parameter values. The decrease in the primary velocity as the Hartman number (M) increases is because the presence of a magnetic field in an electrically conducting fluid introduces a force called the Lorentz force, which acts against the flow if the magnetic field is applied in the normal direction, as in the present study. This resistive force slows down the fluid velocity component as shown in figure 1. The effect of Hall parameter m on the primary velocity flow field is presented in the figure 2 in case of cooling of the plate. Here, the primary velocity profiles are drawn against  $\eta$  for three different values of m. The Hall parameter is found to accelerate the primary velocity of the flow field as m increases. The effect of schmidt number on primary velocity profiles in presence of foreign species such as H<sub>2</sub> (Sc=0.22), Water vapour (Sc=0.60), NH<sub>3</sub> (Sc = 0.78) and Methanol (Sc = 1.00) are shown in figure (3) in case of cooling of the plate and the flow field suffers a decrease in primary velocity at all points in presence of heavier diffusing species. The effects of the thermal radiation parameter F on the primary velocity profiles in the boundary layer is illustrated in figure (4) in case of cooling of the plate. Increasing the thermal radiation parameter F produces significant decrease in the thermal condition of the fluid and its thermal boundary layer. From figure (5) depicts the effect of frequency parameter ( $\Omega$ ) on the primary velocity of the flow field in case of cooling of the plate. Here, the primary velocity profiles are drawn against  $\eta$  for three different values of  $\Omega$ . The frequency parameter is found to decelerate the primary velocity of the flow field at all points. In the figures (1) – (5) on primary velocity profiles are mentioned above, compare to the case of cooling of the plate opposite effects are observed in the case of heating of the plate.

Figures 6 to 10 depicts that the secondary velocity profiles w against  $\eta$  for cooling ( $Gr > 0$ ) and heating ( $Gr < 0$ ) of the plate by free-convection currents taking different values of F (radiation parameter), Sc (Schmidt number), M (Hartmann number), m (Hall parameter) and  $\Omega$  (Frequency parameter). Figure (6) is depicts that the effect of Hartmann number (M) on the secondary velocity of the flow field in case of cooling of the plate. Here, the secondary velocity profiles are drawn against  $\eta$  for three different values of M. The Hartmann number is found to accelerate the secondary

velocity of the flow field at all points. The effect of hall parameter  $m$  on the secondary velocity flow field is presented in the figure (7) in case of cooling of the plate. Here, the secondary velocity profiles are drawn against  $\eta$  for three different values of  $m$ . The hall parameter is found to accelerate the secondary velocity of the flow field at all points. The effect of Schmidt number on secondary velocity profiles in presence of foreign species such as  $H_2$  ( $Sc = 0.22$ ), Water vapour ( $Sc = 0.60$ ),  $NH_3$  ( $Sc = 0.78$ ) and Methanol ( $Sc = 1.00$ ) are shown in figure (8) in case of cooling of the plate. The flow field suffers a decrease in secondary velocity at all points in presence of heavier diffusing species.

The effect of radiation parameter  $F$  on the secondary velocity flow field is presented in the figure (9) in case of cooling of the plate. Here, the secondary velocity profiles are drawn against  $\eta$  for three different values of  $F$ . The radiation parameter is found to decrease the secondary velocity of the flow field at all points. Higher the radiation parameter, the more sharper is the reduction in the secondary velocity. Figure (10) depicts the effect of frequency parameter  $\Omega$  on the secondary velocity of the flow field in case of cooling of the plate. Here, the secondary velocity profiles are drawn against  $\eta$  for three different values of  $\Omega$ . The frequency parameter is found to decelerate the secondary velocity of the flow field at all points. In the figures (6) – (10) on secondary velocity profiles are mentioned above, compare to the case of cooling of the plate opposite effects are observed in the case of heating of the plate.

Figures (11) and (12) depict that the temperature profiles  $\theta$  against  $\eta$  taking different values of  $F$  (radiation parameter) and  $Pr$  (Prandtl number). The thermal boundary layer thickness is greater for fluids with small Prandtl number. The reason is that smaller values of  $Pr$  are equivalent to increasing thermal conductivity and therefore heat is able to diffuse away from the heated surface more rapidly than for higher values of  $Pr$ . Moreover, the effect of radiation is to increase the rate of energy transport to the fluid and accordingly increase the fluid temperature. Figure (13) displays concentration profiles  $C$  vs.  $\eta$  for various gases like Hydrogen ( $Sc = 0.22$ ), Water vapour ( $Sc = 0.60$ ), Oxygen ( $Sc = 0.66$ ) and Ammonia ( $Sc = 0.78$ ) taking  $t = 1$ . It is reported that the effect of increasing values of Schmidt number ( $Sc$ ) is to decrease the concentration profiles. This is consistent with the fact that the increase of  $Sc$  means a decrease of molecular diffusivity ( $D$ ) that result in decrease of concentration boundary layer. Hence the concentration of species is higher for smaller value of  $Sc$  and lower for larger value of  $Sc$ .

Figure (14) shows that an increasing the chemical reaction parameter  $k_r$  the primary velocity profiles are decreasing. It should be mentioned that the studied case is for a destructive chemical reaction ( $k_r$ ). In fact, as chemical reaction ( $k_r$ ) increases, the considerable reduction in the primary velocity profiles is predicted, and the presence of the peak indicates that the maximum value of the velocity occurs in the body of the fluid close to the surface but not at the surface. Figure (15) shows the effect of the chemical reaction parameter  $k_r$  on concentration profiles. As expected, the presence of the chemical reaction significantly affects the concentration profiles. It should be mentioned that the studied case is for a destructive chemical reaction  $k_r$ . In fact, as chemical reaction  $k_r$  increases, the concentration decreases. It is evident that the increase in the chemical reaction  $k_r$  significantly alters the concentration boundary layer thickness but does not alter the momentum boundary layers.

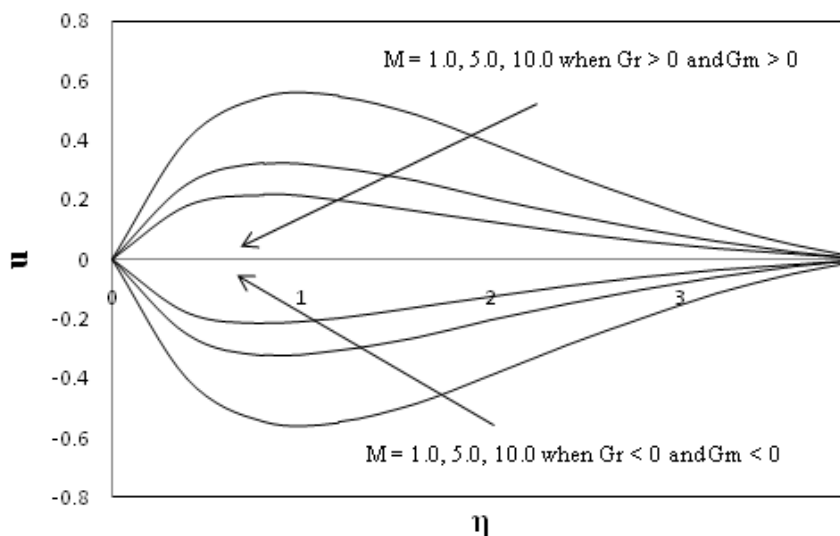


**Figure 1:** Effect of Hartmann number ‘M’ on primary velocity profiles ‘u’ for cooling ( $Gr = 5.0$  &  $Gm = 5.0$ ) and heating of the plate ( $Gr = -5.0$  &  $Gm = -5.0$ ) when  $m = 0.5$ ,  $Sc = 0.22$ ,  $Pr = 0.71$ ,  $F = 1.0$ ,  $\Omega = 1.0$  and  $\Omega t = \pi/2$ .

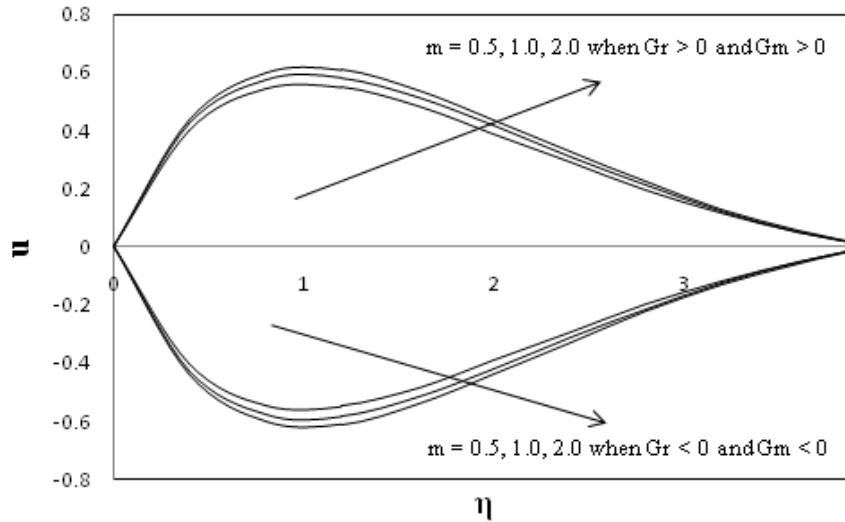


**Figure 2:** Effect of Hall parameter 'm' on primary velocity profiles 'u' for cooling ( $Gr = 5.0$  &  $Gm = 5.0$ ) and heating of the plate ( $Gr = -5.0$  &  $Gm = -5.0$ ) when  $M = 1.0$ ,  $Sc = 0.22$ ,  $Pr = 0.71$ ,  $F = 1.0$ ,  $\Omega = 1.0$  and  $\Omega t = \pi/2$ .

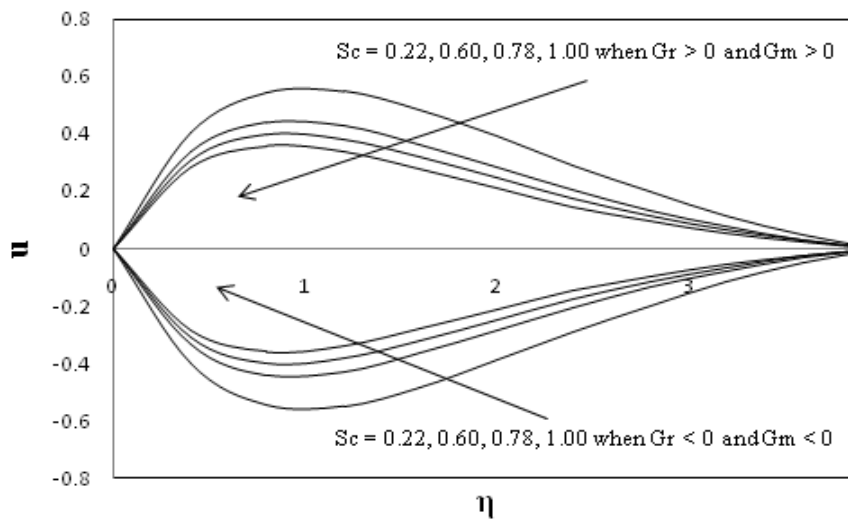


**Figure 3:** Effect of Schmidt number 'Sc' on primary velocity profiles 'u' for cooling ( $Gr = 5.0$  &  $Gm = 5.0$ ) and heating of the plate ( $Gr = -5.0$  &  $Gm = -5.0$ ) when  $m = 0.5$ ,  $M = 1.0$ ,  $Pr = 0.71$ ,  $F = 1.0$ ,  $\Omega = 1.0$  and  $\Omega t = \pi/2$ .

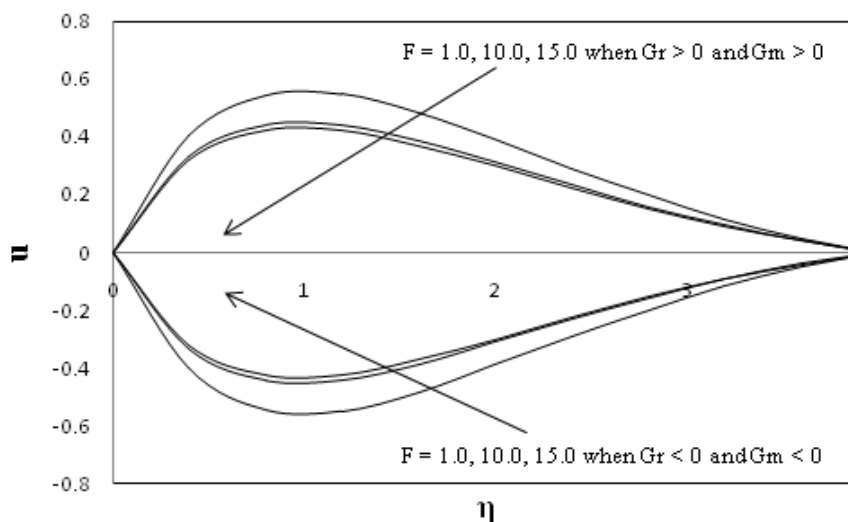


**Figure 4:** Effect of Radiation parameter 'F' on primary velocity profiles 'u' for cooling ( $Gr = 5.0$  &  $Gm = 5.0$ ) and heating of the plate ( $Gr = -5.0$  &  $Gm = -5.0$ ) when  $m = 0.5$ ,  $Sc = 0.22$ ,  $Pr = 0.71$ ,  $M = 1.0$ ,  $\Omega = 1.0$  and  $\Omega t = \pi/2$ .



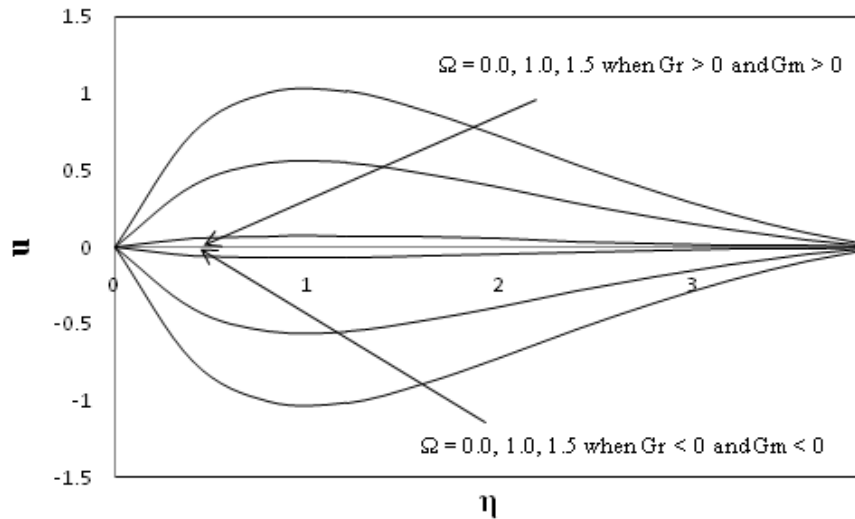


**Figure 5:** Effect of Frequency parameter ' $\Omega$ ' on primary velocity profiles ' $u$ ' for cooling ( $Gr = 5.0$  &  $Gm = 5.0$ ) and heating of the plate ( $Gr = -5.0$  &  $Gm = -5.0$ ) when  $m = 0.5$ ,  $Sc = 0.22$ ,  $Pr = 0.71$ ,  $F = 1.0$ ,  $M = 1.0$  and  $\Omega t = \pi/2$ .

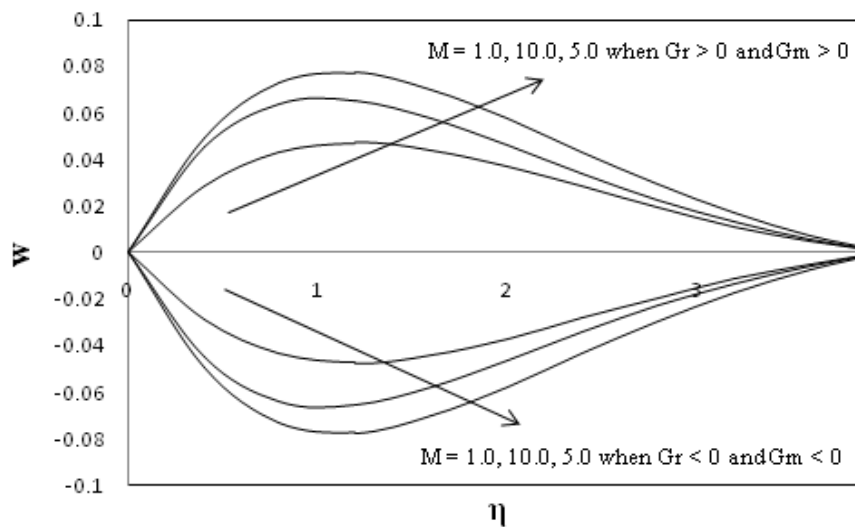


**Figure 6:** Effect of Hartmann number ' $M$ ' on secondary velocity profiles ' $w$ ' for cooling ( $Gr = 5.0$  &  $Gm = 5.0$ ) and heating of the plate ( $Gr = -5.0$  &  $Gm = -5.0$ ) when  $m = 0.5$ ,  $Sc = 0.22$ ,  $Pr = 0.71$ ,  $F = 1.0$ ,  $\Omega = 1.0$  and  $\Omega t = \pi/2$ .

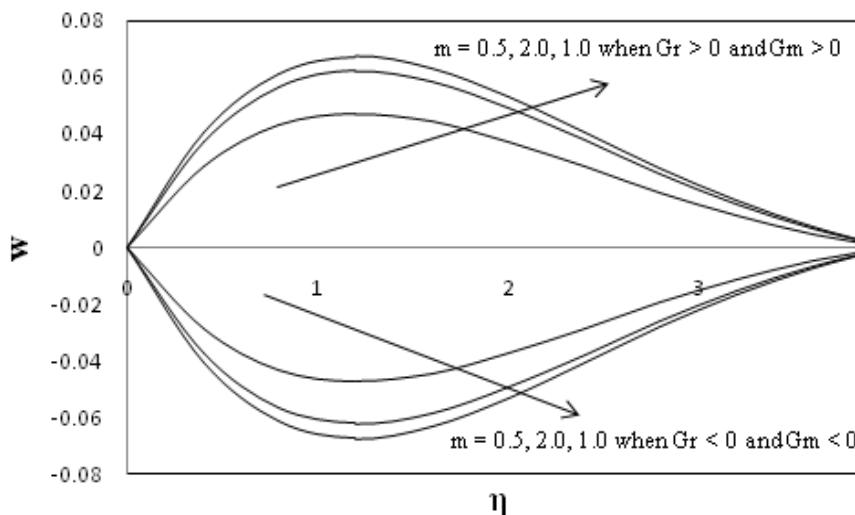


**Figure 7:** Effect of Hall parameter ' $m$ ' on secondary velocity profiles ' $w$ ' for cooling ( $Gr = 5.0$  &  $Gm = 5.0$ ) and heating of the plate ( $Gr = -5.0$  &  $Gm = -5.0$ ) when  $M = 1.0$ ,  $Sc = 0.22$ ,  $Pr = 0.71$ ,  $F = 1.0$ ,  $\Omega = 1.0$  and  $\Omega t = \pi/2$ .

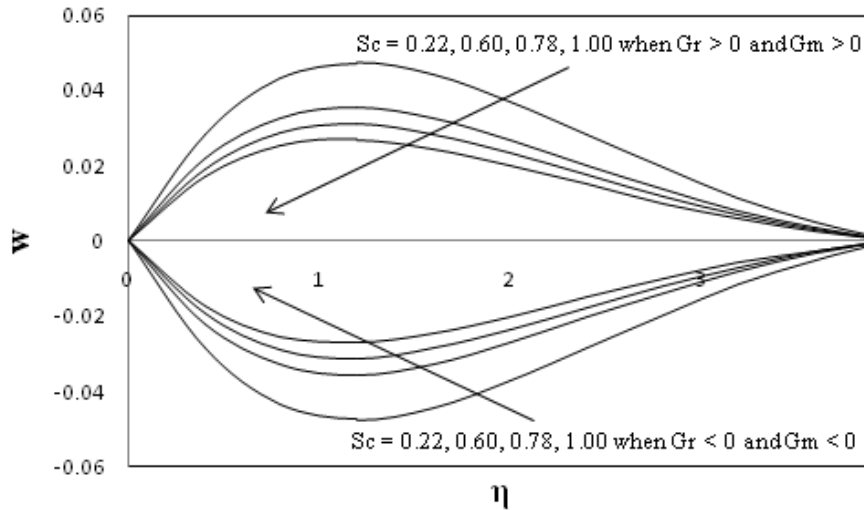


**Figure 8:** Effect of Schmidt number 'Sc' on secondary velocity profiles 'w' for cooling ( $Gr = 5.0$  &  $Gm = 5.0$ ) and heating of the plate ( $Gr = -5.0$  &  $Gm = -5.0$ ) when  $m = 0.5$ ,  $M = 1.0$ ,  $Pr = 0.71$ ,  $F = 1.0$ ,  $\Omega = 1.0$  and  $\Omega t = \pi/2$ .

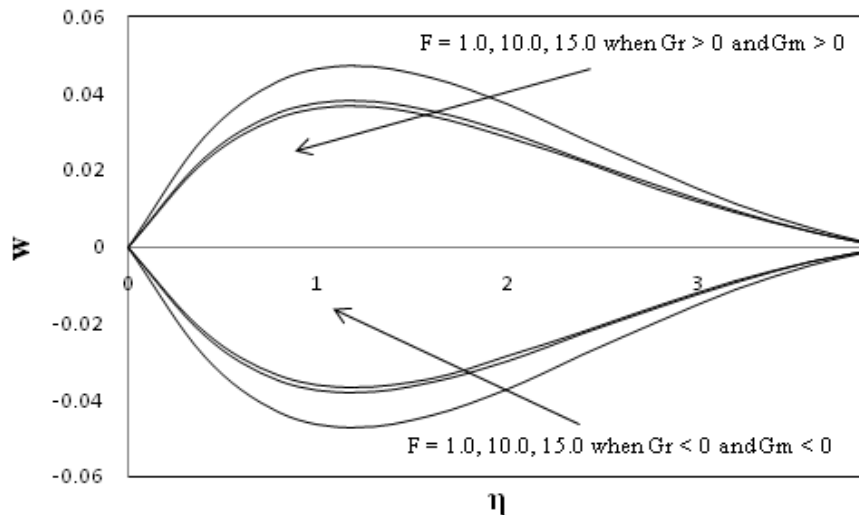


**Figure 9:** Effect of Radiation parameter 'F' on secondary velocity profiles 'w' for cooling ( $Gr = 5.0$  &  $Gm = 5.0$ ) and heating of the plate ( $Gr = -5.0$  &  $Gm = -5.0$ ) when  $m = 0.5$ ,  $Sc = 0.22$ ,  $Pr = 0.71$ ,  $M = 1.0$ ,  $\Omega = 1.0$  and  $\Omega t = \pi/2$ .

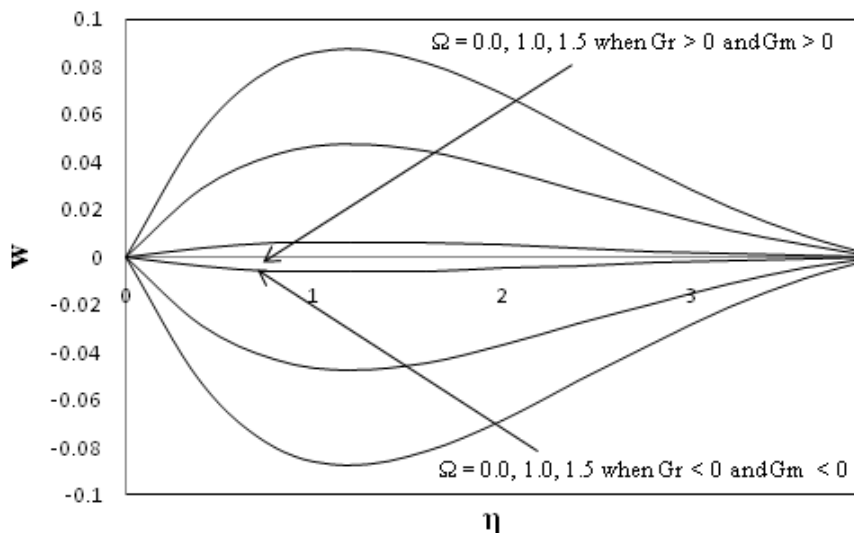


**Figure 10:** Effect of Frequency parameter ' $\Omega$ ' on secondary velocity profiles 'w' for cooling ( $Gr = 5.0$  &  $Gm = 5.0$ ) and heating of the plate ( $Gr = -5.0$  &  $Gm = -5.0$ ) when  $m = 0.5$ ,  $Sc = 0.22$ ,  $Pr = 0.71$ ,  $F = 1.0$ ,  $M = 1.0$  and  $\Omega t = \pi/2$ .

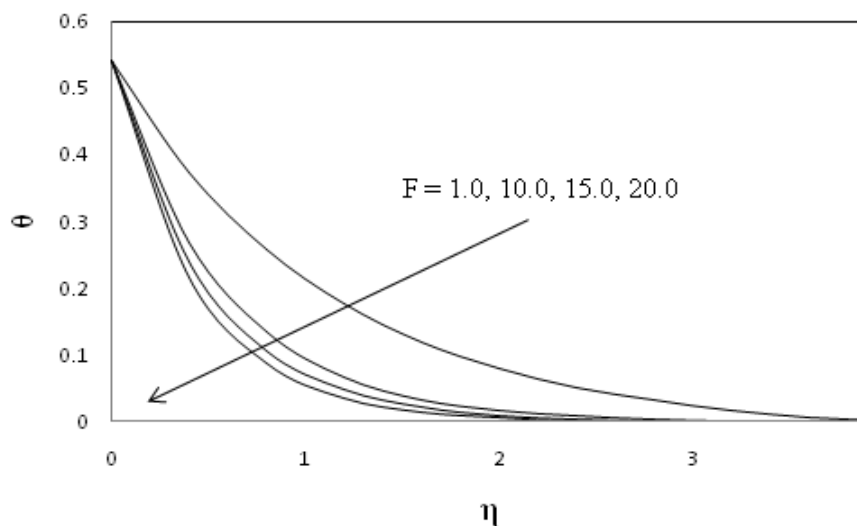


**Figure 11:** Effect of Radiation parameter 'F' on temperature profiles ' $\theta$ ' when  $Gr = 5.0, Gm = 5.0, \Omega = 1.0, Sc = 0.22, Pr = 0.71, m = 0.5, M = 1.0$  and  $\Omega t = \pi/2$ .

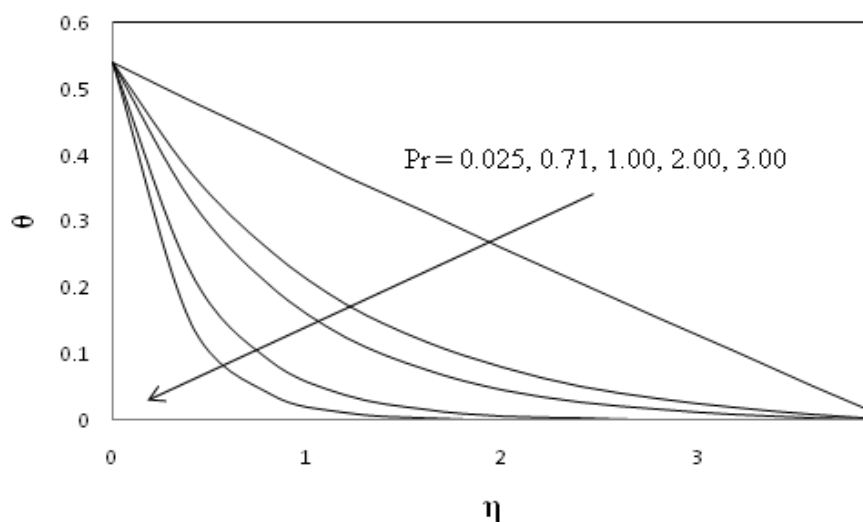


**Figure 12:** Effect of Prandtl number 'Pr' on temperature profiles ' $\theta$ ' when  $Gr = 5.0, Gm = 5.0, \Omega = 1.0, Sc = 0.22, F = 1.0, m = 0.5, M = 1.0$  and  $\Omega t = \pi/2$ .

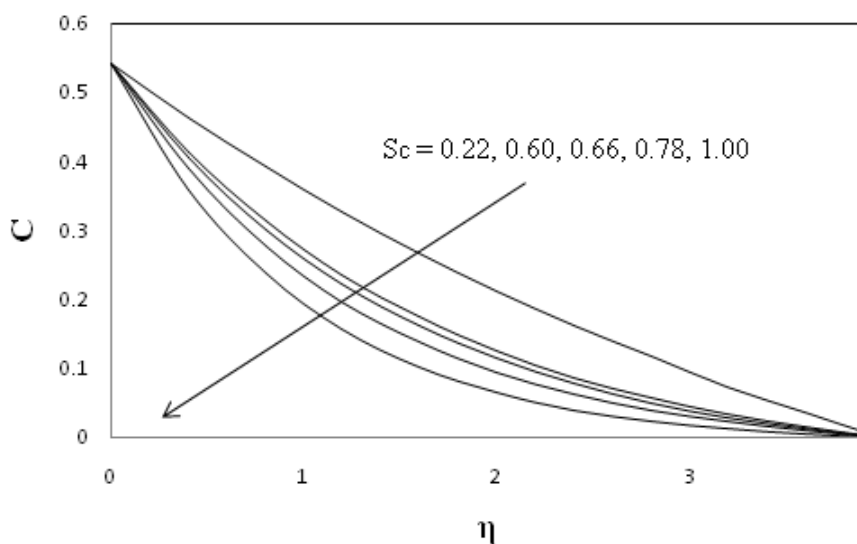


**Figure 13:** Effect of Schmidt number 'Sc' on concentration profiles ' $C$ '

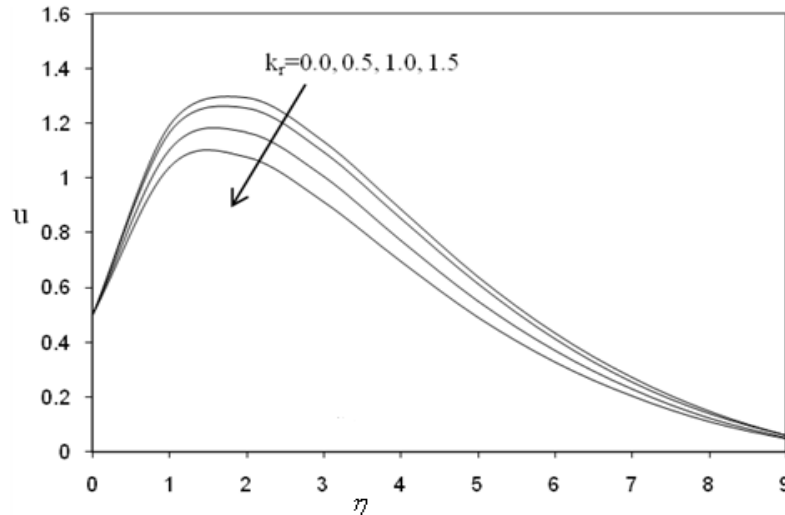


**Figure 14:** Effect of chemical reaction parameter  $k_r$  on primary velocity profile 'u' when  $Gr = 5.0$ ,  $Gm = 5.0$ ,  $\Omega = 1.0$ ,  $Sc = 0.22$ ,  $F = 1.0$ ,  $m = 0.5$ ,  $M = 1.0$  and  $\Omega t = \pi/2$ .

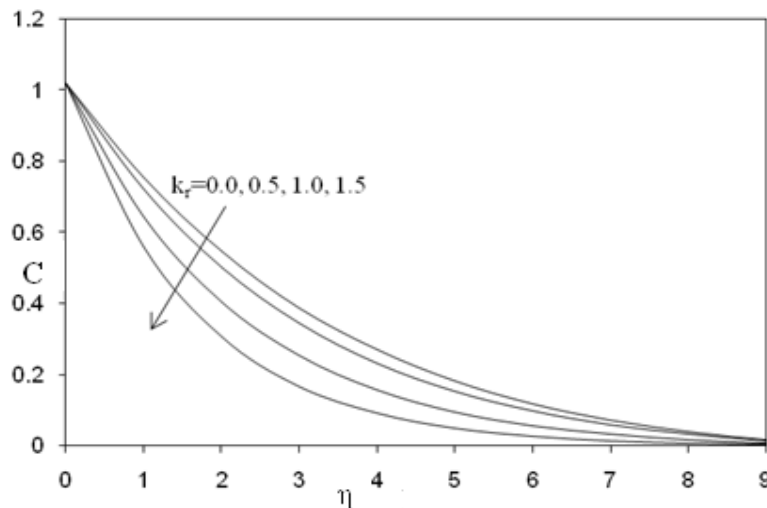


**Figure 15:** Effect of chemical reaction parameter  $k_r$  on concentration profiles 'C' when  $Gr = 5.0$ ,  $Gm = 5.0$ ,  $\Omega = 1.0$ ,  $Sc = 0.22$ ,  $F = 1.0$ ,  $m = 0.5$ ,  $M = 1.0$  and  $\Omega t = \pi/2$ .

Table – 1 presents numerical values of the skin-friction coefficients ( $\tau_1$  &  $\tau_2$ ) for variations in  $Gr$ ,  $Gm$ ,  $m$ ,  $Pr$ ,  $Sc$ ,  $\Omega$  and  $F$  for externally cooling of the plate ( $Gr > 0$ ). It is observed that, an increase in the Prandtl number or Schmidt number or frequency parameter or radiation parameter leads to decrease in the value of skin-friction coefficients while an increase in the Hall parameter or Grashof number or modified Grashof number leads to increase in the value of skin-friction coefficients. The velocity in primary flows decreases with increasing  $M$  therefore  $\tau_1$  also decreases as  $M$  increases. Since, the friction decreases as the fluid velocity decreases. Similarly, the velocity in secondary flows increases as  $M$  increases therefore  $\tau_2$  also exhibits similar behaviour for increasing  $M$ .

**Table-1:** Skin-friction coefficient for cooling of the plate

Gr	Gm	M	m	Sc	Pr	F	$\Omega$	$\tau_1$	$\tau_2$
5.0	5.0	1.0	0.5	0.22	0.71	1.0	1.0	1.3441	0.0867
10.0	5.0	1.0	0.5	0.22	0.71	1.0	1.0	1.8607	0.1150
5.0	10.0	1.0	0.5	0.22	0.71	1.0	1.0	2.1716	0.1450
5.0	5.0	2.0	0.5	0.22	0.71	1.0	1.0	1.1850	0.1247
5.0	5.0	1.0	1.0	0.22	0.71	1.0	1.0	1.4071	0.1232
5.0	5.0	1.0	0.5	0.60	0.71	1.0	1.0	1.1510	0.0673
5.0	5.0	1.0	0.5	0.22	7.00	1.0	1.0	0.8824	0.0590
5.0	5.0	1.0	0.5	0.22	0.71	10.0	1.0	1.1293	0.0699
5.0	5.0	1.0	0.5	0.22	0.71	1.0	1.5	0.1760	0.0113

Table – 2 presents numerical values of the skin-friction coefficients ( $\tau_1$  &  $\tau_2$ ) for variations in Gr, Gm, m, Pr, Sc,  $\Omega$  and F for externally heating of the plate ( $Gr < 0$ ). It is observed that, an increase in the Schmidt number or frequency parameter leads to decrease in the value of skin-friction coefficients while an increase in the Prandtl number or Hall parameter or Grashof number or modified Grashof number or radiation parameter leads to increase in the value of skin-friction coefficients. The velocity in primary flows decreases with increasing M therefore  $\tau_1$  also decreases as M increases. Since, the friction decreases as the fluid velocity decreases. Similarly, the velocity in secondary flows increases as M increases therefore  $\tau_2$  also exhibits similar behaviour for increasing M.

**Table-2:** Skin-friction coefficient for heating of the plate

Gr	Gm	M	m	Sc	Pr	F	$\Omega$	$\tau_1$	$\tau_2$
-5.0	5.0	1.0	0.5	0.22	0.71	1.0	1.0	0.3109	0.0300
-10.0	5.0	1.0	0.5	0.22	0.71	1.0	1.0	-0.2057	0.0016
-5.0	10.0	1.0	0.5	0.22	0.71	1.0	1.0	1.1384	0.0883
-5.0	5.0	2.0	0.5	0.22	0.71	1.0	1.0	0.2563	0.0416
-5.0	5.0	1.0	1.0	0.22	0.71	1.0	1.0	0.3326	0.0431
-5.0	5.0	1.0	0.5	0.60	0.71	1.0	1.0	0.1178	0.0106
-5.0	5.0	1.0	0.5	0.22	7.00	1.0	1.0	0.7726	0.0576
-5.0	5.0	1.0	0.5	0.22	0.71	10.0	1.0	0.5257	0.0467
-5.0	5.0	1.0	0.5	0.22	0.71	1.0	1.5	0.0407	0.0039

The quantity of heat exchanged between the body and the fluid is given by temperature gradient Nu (Nusselt number) which is given in the table – 3. Table – 3 presents numerical values of heat transfer coefficient in terms of Nusselt number (Nu) for different values of the Prandtl number Pr, Radiation parameter F and Frequency parameter  $\Omega$  respectively. It is observed that an increase in the frequency parameter leads to increase in the value of heat transfer coefficient while an increase in the Prandtl number or radiation parameter leads to decrease in the value of heat transfer coefficient.

**Table-3:** Heat transfer coefficient in terms of Nusselt number

Pr	F	$\Omega$	Nu
0.71	1.0	1.0	-0.4753
7.00	1.0	1.0	-2.8696
0.71	10.0	1.0	-0.8613
0.71	1.0	1.5	-0.0692

Table - 4 presents numerical values of mass transfer coefficient in terms of Sherwood number (Sh) for different values of Schmidt number Sc, Chemical reaction parameter  $k_r$  and frequency parameter  $\Omega$  respectively. It is observed that an increase in the Schmidt number leads to decrease in the value of mass transfer coefficient while an increase in the chemical reaction parameter and frequency parameter leads to increase in the value of mass transfer coefficient.

**Table-4:** Mass transfer coefficient in terms of Sherwood number

Sc	$k_r$	$\Omega$	Sh
0.22	0.5	1.0	-0.2009
0.60	0.5	1.0	-0.3461
0.22	1.0	1.0	-0.1028
0.22	0.5	1.5	-0.0263

## ACKNOWLEDGMENT

This research is carried out under the UGC Minor research Project (MRP-4619/14(SERO/UGC)). The Authors are thankful to UGC for financial support.

## REFERENCES

1. J. Anand Rao, S. Sivaiah and R. Srinivasa Raju (2012): Chemical Reaction Effects on an Unsteady MHD Free Convection Fluid Flow past a Semi-Infinite Vertical Plate Embedded in a Porous Medium with Heat Absorption, Journal of Applied Fluid Mechanics, Vol. 5, No. 3, pp. 63-70.
2. S. Ahmed and K. Kalita (2013): Analytical and Numerical Study for MHD Radiating Flow over an Infinite Vertical Surface Bounded by a Porous Medium in Presence of Chemical Reaction, Journal of Applied Fluid Mechanics, Vol. 6, No. 4, pp. 597-607.

3. B. Venkateswarlu and P. V. Satya Narayana (2015): Chemical reaction and radiation absorption effects on the flow and heat transfer of a nanofluid in a rotating system, *Appl Nanosci*, 5:351–360.
4. R. Srinivasa Raju, G. Aruna, N. Swamy Naidu, S. V. K. Varma, and M. M. Rashidi (2016): Chemically reacting fluid flow induced by an exponentially accelerated infinite vertical plate in a magnetic field and variable temperature via LTT and FEM, *Theoretical And Applied Mechanics*, Volume 43, Issue 1, 49–83.
5. F.S. Ibrahim, A.M. Elaiw and A.A. Bakr (2008): Effect of the chemical reaction and radiation absorption on the unsteady MHD free convection flow past a semi infinite vertical permeable moving plate with heat source and suction, *Communications in Nonlinear Science and Numerical Simulation* 13, 1056–1066.
6. B. R. Rout, S. K. Parida, and H. B. Pattanayak (2014): Effect of Radiation and Chemical Reaction on Natural Convective MHD Flow through a Porous Medium with Double Diffusion, *Journal of Engineering Thermophysics*, Vol. 23, No. 1, pp. 53–65.
7. R.S. Tripathy, G.C. Dash, S.R. Mishra, and S. Baag (2015): Chemical reaction effect on MHD free convective surface over a moving vertical plate through porous medium, *Alexandria Engineering Journal*, Volume 54, Issue 3, Pages 673–679.
8. P.V.Satya Narayana and D.HarishBabu(2015): Numerical study of MHD heat and mass transfer of a Jeffrey fluid over a stretching sheet with chemical reaction and thermal radiation, *Journal of the Taiwan Institute of Chemical Engineers*, 1–8.
9. Soundalgekar, V.M. (1977): Free convection effects on the Stokes problem for an infinite vertical plate. *Transactions of the ASME Journal of Heat Transfer*, Vol. 99, pp.499-501.
10. Soundalgekar, V.M. and Wavre, P.D. (1977): Unsteady free convection flow past an infinite vertical plate with constant suction and mass transfer. *Int. J. Heat Mass Transfer*, Vol.20, pp.1363-1373.
11. Perdikis, C. (1986): Free convection and mass transfer effects on the flow past a vertical plate. *Astrophysics and Space Science*, Vol. 119, pp.295-303
12. Lin, H.T. and Wu, C.M. (1995): Combined heat and mass transfer by laminar natural convection from a vertical plate. *Heat and Mass Transfer*, Vol.30, pp.369-376
13. Helmy, K.A. (1999): MHD unsteady free convection flow past a vertical porous plate. *ZAMM*, Vol.78, pp.225-270
14. Acharya, M.; Dash, G.C. and Singh, L.P. (1995): Effect of chemical and thermal diffusion with Hall current on unsteady hydro magnetic flow near an infinite vertical porous plate. *J. Phys. D: Appl. Phys.*, Vol.28, pp. 2455-2464
15. Abo-elahab, E.M. and Elbarbary, E.M.E. (2001): Hall current effect magneto hydrodynamics free convection flow past a semi-infinite vertical plate with mass transfer. *Int. J. Engg. Sci.*, Vol.39, pp.1641-1652
16. Takhar, H.S.; Roy, S. and Nath, G. (2003): Unsteady free convection flow over an infinite vertical porous plate due to the combined effects of thermal and mass diffusion, magnetic field and Hall currents. *Heat and Mass Transfer*, Vol.39, pp.825-834
17. F.M. Ali, R. Nazar, N.M. Arifin and I. Pop (2011): Effect of Hall current on MHD mixed convection boundary layer flow over a stretched vertical flat plate, *Meccanica*, 46:1103–1112.
18. Dulal Pal (2013): Hall current and MHD effects on heat transfer over an unsteady stretching permeable surface with thermal radiation, *Computers and Mathematics with Applications*, Volume 66, Issue 7, Pages 1161-1180.
19. S Sivaiah and R Srinivasa-Raju [2013]: Finite element solution of heat and mass transfer flow with Hall current, heat source, and viscous dissipation, *Applied Mathematics and Mechanics* Volume34, Issue 5, Pages 559-570.
20. Anand Rao, R Srinivasa Raju and S Sivaiah [2012]: Finite element solution of MHD transient flow past an impulsively started infinite horizontal porous plate in a rotating fluid with hall current, *Journal Journal of Applied Fluid Mechanics*, Volume 5, Issue 3, Pages 105-112.
21. G.S. Seth, B. Kumbhakar and R. Sharma [2016]: Unsteady MHD free convection flow with Hall effect of a radiating and heat absorbing fluid past a moving vertical plate with variable ramped temperature, *Journal of the Egyptian Mathematical Society* 24, 471–478.
22. S. Das, S.K. Guchhait, R.N. Jana and O.D. Makinde [2014]: Hall effects on an unsteady magneto-convection and radiative heat transfer past a porous plate, *Alexandria Engineering Journal* 55, 1321–1331.
23. Hossain, M.A. and Takhar, H.S. (1996): Radiation effect on mixed convection along a vertical plate with uniform surface temperature. *Heat and Mass Transfer*, Vol.31, pp.243-248
24. Abo-elahab, E.M. (2004): The effects of temperature-dependent fluid properties on free convective flow along a semi-infinite vertical plate by the presence of radiation. *Heat and Mass Transfer*, Vol.41, pp.163-169
25. Muthucumaraswamy, R. and Kumar, G.S. (2004): Heat and mass transfer effects on moving vertical plate in the presence of thermal radiation. *Theoret. Appl. Mech.*, Vol.31, pp.35-46.
26. N. Vedavathi, K. Ramakrishna and K. Jayarami Reddy [2015] : Radiation and mass transfer effects on unsteady MHD convective flow past an infinite vertical plate with Dufour and Soret effects, *Ain Shams Engineering Journal* 6, 363–371.
27. R.N. Barik and G.C. Dash [2014]: Thermal radiation effect on an unsteady magnetohydrodynamic flow past inclined porous heated plate in the presence of chemical reaction and viscous dissipation, *Applied Mathematics and Computation* 226, 423–434.

28. J. Prakash, D. Bhanumathi, A. G. Vijaya Kumar and S. V. K. Varma [2014]: Diffusion-Thermo and Radiation Effects on Unsteady MHD Flow Through Porous Medium Past an Impulsively Started Infinite Vertical Plate with Variable Temperature and Mass Diffusion, *Transp Porous Med* 96:135–151.
29. F.I. Alao, A.I. Fagbade and B.O. Falodun [2016]: Effects of thermal radiation, Soret and Dufour on an unsteady heat and mass transfer flow of a chemically reacting fluid past a semi-infinite vertical plate with viscous dissipation, *Journal of the Nigerian Mathematical Society* 35, 142–158.

**Source of support: Nil, Conflict of interest: None Declared**

***[Copy right © 2016. This is an Open Access article distributed under the terms of the International Journal of Mathematical Archive (IJMA), which permits unrestricted use, distribution, and reproduction in any medium, provided the original work is properly cited.]***